Low-lying phonon dispersion curves of $D0_3$ Cu$_3$Al(+Be)

Lluís Mañosa

Departament d'Estructura i Constituents de la Matèria, Facultat de Física, Universitat de Barcelona, Diagonal 647,
E-08028 Barcelona, Catalonia, Spain

J. Zarestky, M. Bullock, and C. Stassis

Ames Laboratory and Department of Physics and Astronomy, Iowa State University, Ames, Iowa 50011
(Received 4 December 1997; revised manuscript received 3 December 1998)

The low-lying phonon dispersion curves of a $D0_3$ ordered Cu$_3$Al(+Be) shape-memory alloy were measured, at room temperature, along the $[\xi 00]$, $[\xi\xi 0]$, $[\xi\xi\xi]$, $[\xi\xi 1]$, and $[\frac{1}{2}, \frac{1}{2}, \xi]$ symmetry directions. As in other bcc metals and alloys, we find that the frequencies of the $TA_2[\xi\xi 0]$ modes are relatively low and that the $L[\xi\xi\xi]$ branch exhibits a pronounced dip at $\xi = \frac{2}{3}$. The measured low-lying phonon dispersion curves are quite similar to those of a bcc structure. Actually, a fifth-nearest-neighbor force constant bcc model provides a satisfactory fit to the low-lying phonon dispersion curves of this alloy. This model was used to evaluate the elastic constants, the phonon density of states, and the lattice specific heat. The results of these calculations are in good agreement with macroscopic measurements of the elastic constants and specific heat of this alloy. [S0163-1829(99)02114-1]

I. INTRODUCTION

Many bcc metals and alloys undergo a first-order martensitic phase transition to a close-packed phase.[1] Because of their shape-memory properties, noble-metal-based alloys are of particular interest. Cu-based alloys belong to this family of compounds and have received, in recent years, considerable attention. These alloys are Hume-Rothery phases for which the phase stability is governed by the concentration of valence electrons.[2] The bcc structure is only stable at high temperature (usually above ~700–800 K), but by means of a sufficiently rapid cooling, it is possible to retain the bcc structure in a metastable state at lower temperatures. This relatively low-temperature metastable bcc phase usually exhibits long-range atomic order. The most common ordered structures are the $B2$ ($Pm3m$) and $D0_3$ or $L2_1$ ($Fm3m$) structures.[3] Upon further cooling, the alloys transform martensitically to the low-temperature phase. An important feature of the Cu-based alloys is that the addition of small amounts of a third alloying element (such as Be) makes it possible to obtain alloys with a broad range of martensitic transition temperatures.

In this paper we present the results of an inelastic neutron-scattering study of only the low-lying (less than approximately 25 meV) vibrational modes of Cu$_3$Al(+Be) alloy at room temperature, because one may expect these acoustic branches to resemble those of a bcc lattice. At room temperature this alloy exhibits the $D0_3$ ordered structure[4] which is based on the bcc structure. The conventional unit cell contains eight bcc cells and the lattice parameter is doubled. The addition of a small amount of beryllium to the stoichiometric Cu$_3$Al does not modify significantly the position of the eutectoid point in the equilibrium phase diagram,[5] and the order-disorder transition temperature of this ternary alloy is only weakly dependent on the Be. As we already pointed out, on the other hand, the martensitic transition temperature is very sensitive to the Be concentration.[6]

II. EXPERIMENTAL DETAILS

The Cu-Al-Be crystal used in the present experiment was provided to us by M. Morin and S. Belkahla of the Institut des Sciences Appliquées in Lyon (France). The master alloy, from which the crystal was grown, was prepared by adding appropriate quantities of 99.99 wt % pure Cu and Al to a Cu-4.3 wt % Be alloy. The crystal was grown by the Bridgman technique in a quartz crucible. It was homogenized in air at 1120 K, and then quenched in water at 298 K. After quenching the crystal was cleaned with dilute nitric acid. The dimensions of the sample are $9.4 \times 9.4 \times 7.3$ mm^3.

At room temperature the Cu$_{0.7373}$Al$_{0.2272}$Be$_{0.0355}$ crystal has a bcc lattice parameter of 2.90 Å, and it exhibits the $D0_3$ ordered structure, as verified by both x-ray- and neutron-diffraction measurements. The order-disorder and martensitic transition temperature of the sample were determined, by calorimetric measurements, to be 803 and 145 K, respectively. The elastic constants of the sample were obtained by ultrasonic techniques,[7] and in a previous inelastic neutron-scattering experiment[8] we studied the temperature dependence of the $TA_2[110]$ phonon dispersion curve; in this latter study the sample was labeled as crystal "E."

The measurements were performed using the HB1-A and HB-3 triple-axis spectrometers at the High Flux Isotope Reactor (HFIR) of the Oak Ridge National Laboratory. In both spectrometers pyrolitic graphite, reflecting from the (002) planes, was used as monochromator and analyzer. The measurements on HB-1A were performed at a constant incident-neutron energy of 14.7 meV and those on HB-3 at a constant scattered-neutron energy of 30.5 meV. In all measurements, a pyrolitic graphite filter was positioned either before or after the sample to attenuate the higher-order contamination of the beam. In all measurements collimation of 40 min of arc before and after the sample, and 70 min of arc between analyzer and detector was used. Before the monochromator, 40 min of arc and no collimation was used on HB-3 and HB-1A, respectively.

TABLE I. Measured phonon frequencies (meV) of $D0_3$ $Cu_3Al(+Be)$. The $T_2[\xi\xi0]$ data are from a previous investigation (Ref. 8).

ξ	$L[00\zeta]$	ξ	$\Lambda[\xi\xi1]$	ξ	$T_2[\xi\xi0]$	ξ	$T[\xi\xi\xi]$
0.05	4.0±0.1	0.25	23.6±0.2	0.05	1.1±0.1	0.05	2.2±0.1
0.10	7.0±0.1	0.35	25.0±0.3	0.10	2.2±0.1	0.10	4.7±0.1
0.15	10.0±0.1	0.50	20.5±0.3	0.15	3.0±0.1	0.15	6.9±0.1
0.20	12.5±0.1			0.20	3.7±0.1	0.20	9.2±0.1
0.25	14.8±0.1	ζ	$\pi[0.5\ 0.5\ \zeta]$	0.25	4.2±0.1	0.25	11.0±0.1
0.35	18.3±0.1	0.85	7.4±0.1	0.30	4.5±0.1	0.30	14.3±0.2
0.40	19.5±0.2	0.75	9.8±0.3	0.35	4.9±0.1	0.35	15.6±0.1
0.45	20.5±0.1	0.60	17.4±0.2	0.40	5.2±0.1	0.40	17.3±0.4
0.50	20.5±0.2	0.50	19.8±0.3	0.45	5.4±0.1	0.45	18.9±0.1
0.60	21.4±0.1	0.00	5.4±0.1	0.50	5.4±0.1	0.50	20.5±0.1
0.70	21.6±0.1					0.60	23.6±0.2
0.80	22.0±0.1	ζ	$\Lambda[0.5\ 0.5\ \zeta]$	ξ	$T_1[\xi\xi0]$	0.70	24.6±0.3
0.90	21.9±0.1	0.900	19.3±0.4	0.05	3.5±0.1	0.80	23.3±0.6
1.00	21.9±0.2	0.750	19.9±0.3	0.10	7.0±0.1	0.90	23.5±0.2
		0.500	19.8±0.2	0.15	10.1±0.1	1.00	22.8±0.1
ξ	$T[00\xi]$	0.400	19.5±0.2	0.20	13.1±0.1		
0.10	4.8±0.1	0.375	19.9±0.2	0.25	15.9±0.1	ξ	$L[\xi\xi\xi]$
0.15	7.4±0.1	0.250	19.1±0.2	0.30	17.6±0.1	0.05	8.0±0.1
0.25	11.6±0.1	0.125	19.6±0.2	0.40	19.8±0.1	0.10	15.3±0.1
0.35	15.7±0.1	0.000	19.8±0.2	0.45	19.8±0.1	0.15	18.5±0.1
0.40	17.3±0.1			0.50	19.8±0.1	0.20	23.7±0.3
0.50	19.8±0.1	ζ	$\pi[0.5\ 0.5\ \zeta]$			0.25	24.5±0.6
0.60	22.8±0.1	0.500	19.8±0.4	ξ	$L[\xi\xi0]$	0.30	23.1±0.1
0.70	24.3±0.5	0.425	24.4±0.8	0.05	5.6±0.2	0.35	23.7±0.3
0.80	24.3±0.5	0.375	24.5±0.5	0.10	11.0±0.1	0.40	24.5±0.3
0.90	22.1±0.1	0.250	25.2±0.2	0.15	16.3±0.1	0.45	23.8±0.2
1.00	22.2±0.2	0.125	22.8±0.2	0.20	19.3±0.1	0.50	20.0±0.2
		0.000	22.2±0.6	0.25	22.7±0.1	0.55	17.3±0.1
ξ	$\pi[\xi\xi1]$			0.30	24.6±0.1	0.60	14.0±0.2
0.25	16.6±0.3			0.35	24.4±0.3	0.70	15.0±0.2
0.35	12.2±0.1			0.40	23.6±0.5	0.75	14.9±0.2
0.40	9.6±0.1			0.45	23.7±0.8	0.80	17.9±0.2
0.45	6.6±0.1			0.50	22.2±0.5	0.85	20.2±0.1
0.50	5.6±0.1					1.00	20.6±0.2

III. EXPERIMENTAL RESULTS AND DISCUSSION

The measurements were performed at room temperature with the (110) crystal plane oriented to coincide with the (horizontal) scattering plane. The measured phonon frequencies along the main symmetry directions are listed in Table I. The low-lying dispersion curves are quite similar to those of the bcc structure. This can be seen in Fig. 1 where the measured dispersion curves are plotted in the extended zone scheme to emphasize this similarity.

Two features of the measured dispersion curves should be noticed. It can be seen (Fig. 1) that the longitudinal $[\xi\xi\xi]$ branch exhibits a pronounced dip at $\xi=\frac{2}{3}$. This feature is typical of all bcc materials and it is due to their natural instability towards the formation of the ω phase. Also, the frequencies of the $TA_2[110]$ modes are relatively low and,

as we demonstrated in a previous investigation,[8] decrease with decreasing temperature. It should be pointed out that this latter feature is common to many alloys which undergo a martensitic transformation.[9]

The measured phonon frequencies are approximately 10–20 % lower than those[10] of the $D0_3$ ordered Fe_3Al, if one takes into account the differences in mass, lattice constant, and melting temperature of these materials. The frequency of the zone boundary mode of the $TA_2[110]$ branch of Fe_3Al, on the other hand, is more than two times larger than the corresponding frequency in $Cu_3Al(+Be)$. This big difference is most likely the reason why Fe_3Al does not undergo a martensitic transformation.

The data were analyzed by conventional bcc Born–von Kármán models including up to five-nearest-neighbor force
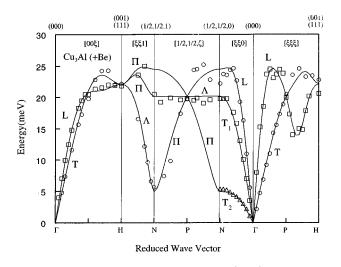
FIG. 1. Phonon dispersion of $D0_3$ Cu$_3$Al(+Be) at room temperature in the extended zone scheme. The solid lines were obtained by fitting the data to a fifth-nearest-neighbor force constant bcc model.
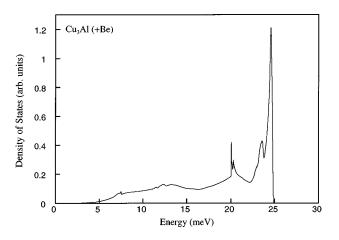

FIG. 2. Partial phonon density of states of $D0_3$ Cu$_3$Al(+Be), calculated using the force constants listed in Table II.

constants. It can be seen (Fig. 1) that a fifth-nearest-neighbor bcc model provides an adequate fit to the experimental data. This is the most important result of the present paper.

The force constants obtained by fitting the data and the elastic constants evaluated using this model are listed in Table II. The elastic constants C' and C_{44} obtained from the fit to the experimental data are in good agreement with the measured elastic constants.[7] The elastic constant C_{11} obtained by the model, on the other hand, is 17% larger than the experimental value and changes considerably as the number of the nearest-neighbor force constants included in the model's increases. A more reliable estimate for this elastic constant can be obtained directly from the slope of the $L[100]$ branch, and this value is in good agreement with the ultrasonic measurements.

The phonon density of states, for the low-lying dispersion curves described by the bcc model, was calculated by the method of Gilat and Raubenheimer[11] and it is plotted in Fig.

2. It can be seen that the various peaks in this partial phonon density of states (Fig. 2) correspond to the high phonon density regions of the dispersion curves, except those in the vicinity of 12 meV. Calculations based on the five-nearest-neighbor force constant model show that these peaks correspond to high phonon density regions of the $TA[\xi\xi 2\xi]$ dispersion curve.

The bcc phonon density of states was used to estimate the lattice contribution to the specific heat of Cu$_3$Al(+Be). The results expressed in terms of an effective Debye temperature θ are plotted in Fig. 3, and the actual values of the calculated specific heat are compared in Fig. 4 with calorimetric measurements of the total specific heat performed, on a small sample (23.5 mg) from the same single crystal, using a modulated differential scanning calorimeter. It is seen (Fig. 4) that the calculated lattice specific heat is in quite good agreement with the total specific heat. This is as expected for the following reasons. First, in the temperature range of the calorimetric measurements the electronic specific heat is negligible compared to the lattice specific heat. Second, in this temperature range, the three relatively high-energy optical modes, not included in the model, do not contribute significantly to the lattice specific heat. Actually, if the small

TABLE II. Longitudinal (l) and transverse (t) axially symmetric force constants obtained by fitting the data to a fifth-nearest-neighbor force constant bcc model. Comparison of the elastic constants derived from the model with ultrasonic measurements (see text).

Shell	r (Å)	# Atoms in shell	l (10^3 dyn/cm)	t (10^3 dyn/cm)
1	2.526	8	7.971	−0.716
2	2.903	6	−0.387	0.607
3	4.105	12	0.767	0.067
4	4.814	24	0.513	−0.266
5	5.028	8	1.003	0.259

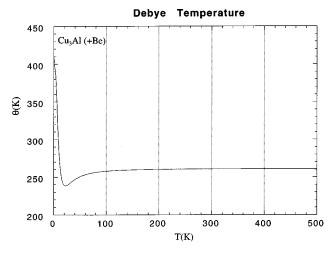|	Elastic constants (GPa)	
	Model	Experiment (Ref. 7)
C_{11}	165	141
C_{44}	83	91
C'	7.49	7.64

FIG. 3. Temperature dependence of the effective Debye temperature, evaluated using the partial phonon density of states plotted in Fig. 2.
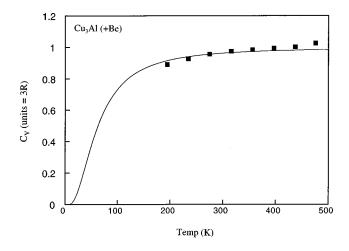
FIG. 4. The lattice specific heat of $Cu_3Al(+Be)$ evaluated using the density of states plotted in Fig. 2. The solid symbols are the values of the total specific heat measured by calorimetric techniques.

deviations of the measured specific heat from the model calculations at temperatures above 400 K (see Fig. 4) can be attributed to the contributions of these three optical modes, we estimate (on the basis of an Einstein model) that these modes must be located at approximately 40 meV. This estimate is consistent with the experimentally measured frequencies of these modes in Fe_3Al.[12]

In summary, we have measured the low-lying phonon dispersion curves of a $D0_3$ ordered $Cu_3Al(+Be)$ shape-memory alloy. We find, in particular, that the low-lying dispersion curves of this Cu-based alloy are (as in the case[10] of Fe_3Al) quite similar to those of a bcc metal. The elastic constants and lattice specific heat, calculated from a Born–von Kármán fit to the data, are in good agreement with macroscopic measurements of these quantities. The results obtained in this experiment can be used, by appropriate scaling, to describe the lattice vibrational properties of other families of Cu-based alloys, since there is considerable evidence[13,14] that these properties are quite similar for these families.

[1] L. Delaey, in *Materials Science and Technology*, edited by P. Haasen (VCH, Weinheim, 1991), Vol. 5, p. 339.

[2] D. Pettifor, *Bonding and Structure of Molecules and Solids* (Clarendon, Oxford, 1995).

[3] M. Ahlers, Prog. Mater. Sci. **30**, 135 (1986).

[4] G. Bester, B. Meyer, and M. Fähnle, Phys. Rev. B **57**, R11 019 (1998).

[5] S. Belkahla and G. Guénin, J. Phys. III **1**, C4 (1991).

[6] M. Jurado, T. Castán, Ll. Mañosa, A. Planes, J. Bassas, X. Alcobé, and M. Morin, Philos. Mag. A **75**, 1237 (1997).

[7] A. Planes, Ll. Mañosa, D. Ríos-Jara, and J. Ortín, Phys. Rev. B **45**, 7633 (1992).

[8] Ll. Mañosa, J. Zarestky, T. Lograsso, D. W. Delaney, and C. Stassis, Phys. Rev. B **48**, 15 708 (1993).

[9] A. Nagasawa and Y. Morii, Mater. Trans., JIM **34**, 855 (1993).

[10] I. M. Robertson, J. Phys.: Condens. Matter **3**, 8181 (1991).

[11] G. Gilat and L. J. Raubenheimer, Phys. Rev. **144**, 390 (1966).

[12] C. Van Dijk, Phys. Lett. **32A**, 255 (1970).

[13] R. Romero and J. L. Pelegrina, Phys. Rev. B **50**, 9046 (1994).

[14] A. Planes, Ll. Mañosa, and E. Vives, Phys. Rev. B **53**, 3039 (1996).